LHC PHENOMENOLOGY WITH KrkNLO MATCHING*

Pratixan Sarmah, Andrzej Siódmok, James Whitehead

Institute of Applied Computer Science, Jagiellonian University
Łojasiewicza 11, 30-348 Kraków, Poland

Received 14 April 2025, accepted 21 April 2025,
published online 26 June 2025

Next-to-leading order (NLO) QCD predictions coupled with parton showers, known as NLO matching, have been widely used for the precision era at the LHC. While two methods — Mc@Nlo and Powheg — have been widely adopted for this purpose, a third method, KrkNLO, has recently been described and implemented within Herwig 7 for colour-singlet processes. We present phenomenological results of this method for the charged-current Drell–Yan process and compare with the Mc@Nlo method.

DOI:10.5506/APhysPolBSupp.18.5-A29

1. Introduction

The precision era at LHC has witnessed significant improvements in the accuracy of QCD predictions. As a result, next-to-leading order (NLO) predictions have become the state-of-the-art for many processes and for multiple observables. These predictions are fully automated for inclusive observables and can be used out of the box either through dedicated packages such as MadGraph [1] and OpenLoops [2], or more generally, within Monte Carlo event generators such as PYTHIA [3, 4], Herwig [5–7], and Sherpa [8, 9]. At the same time, advances in logarithmic resummation, particularly in the form of parton shower algorithms, have enabled simulations of exclusive high-multiplicity final states allowing for more accurate predictions of exclusive observables.

It is evident that both the approaches, fixed order NLO calculations and parton shower resummation, are complementary to each other and should give accurate predictions for a wider set of observables across the full phase space when combined. This is achieved by 'NLO Matching' and has been solved in general by the two methods — Mc@Nlo [10] and Powheg [11–13].

* Presented by P. Sarmah at the 31$^{\mathrm{st}}$ Cracow Epiphany Conference on the *Recent LHC Results*, Kraków, Poland, 13–17 January, 2025.

We briefly summarize a third method, the KrkNLO method in Section 2 and present phenomenological results comparing the KrkNLO method with the Mc@Nlo method for the charged-current Drell–Yan process in Section 3.

2. KrkNLO method

The KrkNLO method, introduced in [14–16] and implemented for colour-singlet processes within Herwig 7 in [17], takes advantage of the freedom to choose an appropriate factorisation scheme which then simply achieves the NLO Matching condition with a simple reweighting. The KrkNLO method can be algorithmically summarized as:

---

for all Born events **do** shower
  if emission generated, from kernel (α) **then**
    $w \leftarrow w \times \frac{R(\Phi_{m+1})}{P_m^{(\alpha)}(\Phi_{m+1})}$
  else
    $w \leftarrow w \times \left[1 + \frac{\alpha_{\mathrm{S}}(\mu_{\mathrm{R}})}{2\pi}\left(\frac{V(\Phi_m;\mu_{\mathrm{R}})}{B(\Phi_m)} + \frac{I(\Phi_m;\tilde{\mu}_{\mathrm{R}})}{B(\Phi_m)} + \Delta_0^{\mathrm{FS}}\right)\right]$
  end if
end for

Here, Φ_m denotes the m-particle phase space with $B(\Phi_m)$ and $V(\Phi_m)$ representing the Born and virtual matrix elements. The $(m+1)$-particle phase space is denoted by Φ_{m+1} with $R(\Phi_{m+1})$ representing the real matrix element on this phase space. The splitting kernels are denoted by $P_m^{(\alpha)}$ with (α) denoting the type of splitting, μ_{R} is the renormalisation scale, and $I(\Phi_m)$ represents the contribution from the integration of the shower Sudakov over the radiative phase space $\Phi_{+1}^{(\alpha)}$. This achieves NLO accuracy only when the reweighted partonic cross section is convolved with PDFs in the 'Krk' factorisation scheme [18]. This dependence on the factorisation scheme is encapsulated by the Δ_0^{FS} term which, with the 'Krk' PDFs, effectively cancels the Catani–Seymour P and K operators originating from collinear counter terms.

3. Charged-current Drell–Yan phenomenology

We present here phenomenological results comparing the KrkNLO method with the Mc@Nlo method for the charged-current Drell–Yan process. We use fiducial cuts close to those used by ATLAS for the LHC Run 1 at 7 TeV [19, 20]:

$$p_{\mathrm{T}}^{\ell} > 30\ \mathrm{GeV}\,, \qquad p_{\mathrm{T}}^{\nu} > 25\ \mathrm{GeV}\,, \tag{1a}$$

$$M_{\ell\nu} > 50\ \mathrm{GeV}\,, \qquad |y^{\mathrm{FS}}| \in [0, 5.0)\ , \tag{1b}$$

Generator cuts are chosen such that they are sufficiently inclusive of the fiducial cuts with $p_{\mathrm{T}}^{\ell,\nu} > 15$ GeV for MC@NLO and $p_{\mathrm{T}}^{\ell,\nu} > 1$ GeV for KrkNLO. Additionally, $M_W > 45$ GeV is applied to both the methods. We allow for a wider coverage of the phase space for the KrkNLO method to avoid any migration effects arising from excluded regions. For the MC@NLO method, we consider three different choices of the shower starting scale [17] representing the matching scheme uncertainty intrinsic to the method:

— 'power'-shower with $Q(\Phi_m) = Q_{\max}(\Phi_m)$ and $Q(\Phi_{m+1}) = Q_{\max}(\Phi_{m+1})$;

— 'default' shower with $Q(\Phi_m) = \sqrt{\hat{s}_{12}} \equiv M_W$ and $Q(\Phi_{m+1}) = p_{\mathrm{T}}^{j_1}$, and

— 'DGLAP-inspired' choice in which the shower starting-scale consistently matches the factorisation scale, $Q(\Phi_m) = M_W$ and $Q(\Phi_{m+1}) = M_W$.

For the KrkNLO method, the shower starting scale is fixed to $Q_{\max}(\Phi_m)$ as required for populating the real-emission phase space without dead zones.

3.1. One emission

In Fig. 1, we compare the KrkNLO method with the MC@NLO method for the shower truncated after the first emission. Since we allow for only one emission, the 'default' and 'DGLAP'-inspired choices of MC@NLO runs are identical, therefore, we present only one here. We also present the fixed-order NLO along with the two methods. It can be seen that KrkNLO is suppressed relative to MC@NLO in the low-$p_{\mathrm{T}}^{j_1}$ region of the $p_{\mathrm{T}}^{j_1}$-distribution. This is due to the presence of the Sudakov factor $\Delta\big|_{p_{\mathrm{T},1}}^{Q(\Phi_m)}$ with the real-emission matrix element within the KrkNLO method. In the high-$p_{\mathrm{T}}^{j_1}$ region, the difference between the KrkNLO and the default MC@NLO reduces and they converge to the fixed-order NLO for $p_{\mathrm{T}}^{j_1} > 100$ GeV. The relative suppression of the KrkNLO method in the low-$p_{\mathrm{T}}^{j_1}$ region is also observed in other distributions, such as the M_W distribution where the KrkNLO method lies 10–25% below the other methods. Such differences can also be seen in the y_{j_1} and $p_{\mathrm{T}}^{\ell_1}$-distributions where KrkNLO method lies 10–40% below MC@NLO. We note here that the 'power'-shower MC@NLO diverges significantly in the high-p_{T} regions of $p_{\mathrm{T}}^{j_1}$ and $p_{\mathrm{T}}^{\ell_1}$-distributions due to the availability of additional phase space. However, these differences are negligible in the M_W and y_{j_1}-distributions.

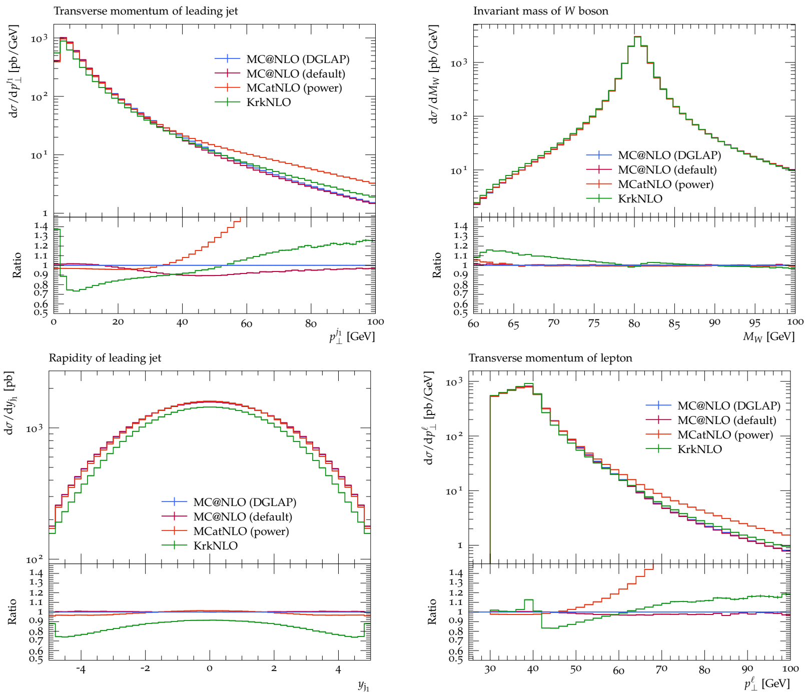

Fig. 1. Parton level (first-emission) comparison of KrkNLO with Mc@Nlo at different shower scales and NLO fixed-order.

3.2. Full shower

In Fig. 2, we compare the KrkNLO method with the three choices of Mc@Nlo method for the shower allowed to run to completion. This provides phenomenologically meaningful comparisons between the two methods. It can be seen that the KrkNLO method is in reasonable agreement with the Mc@Nlo method. As before, the 'power'-shower Mc@Nlo diverges in the high-p_T region as seen in the $p_\mathrm{T}^{j_1}$ and $p_\mathrm{T}^{\ell_1}$-distributions. However, there is virtually no sensitivity to the choice of shower starting scale for the Mc@Nlo method in the M_W and y_{j_1}-distributions. The KrkNLO method lies within the envelope spanned by the Mc@Nlo runs for the p_T-distributions and deviates 10–20% in the M_W and y_{j_1}-distributions.

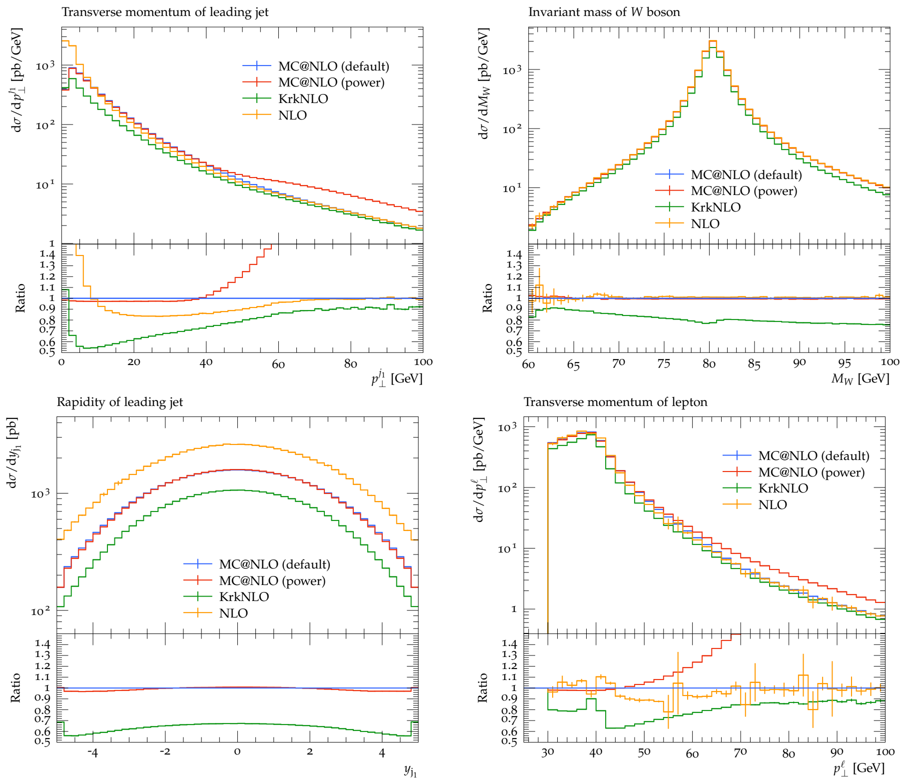

Fig. 2. Parton level (full shower) comparison of KrkNLO with MC@NLO at different shower scales.

3.3. Comparison with ATLAS data

Finally, we compare the KrkNLO and MC@NLO methods to data from ATLAS measurements for LHC Run 1 at 7 TeV in Fig. 3. The results show good agreement of the KrkNLO method along with the MC@NLO method for the $|\eta_\ell|$ and charge asymmtery distributions to within 5%. The phenomenological differences between the methods are more evident in the $p_{\rm T}^j$ and $|y^j|$ distributions, upto 30–40%, as these require higher-order corrections to be formally NLO accurate. Following the trend as seen in Fig. 2 and as discussed in Section 3.2, the 'power'-shower MC@NLO generally lies above the others, while the KrkNLO method lies within the envelope of the different MC@NLO runs.

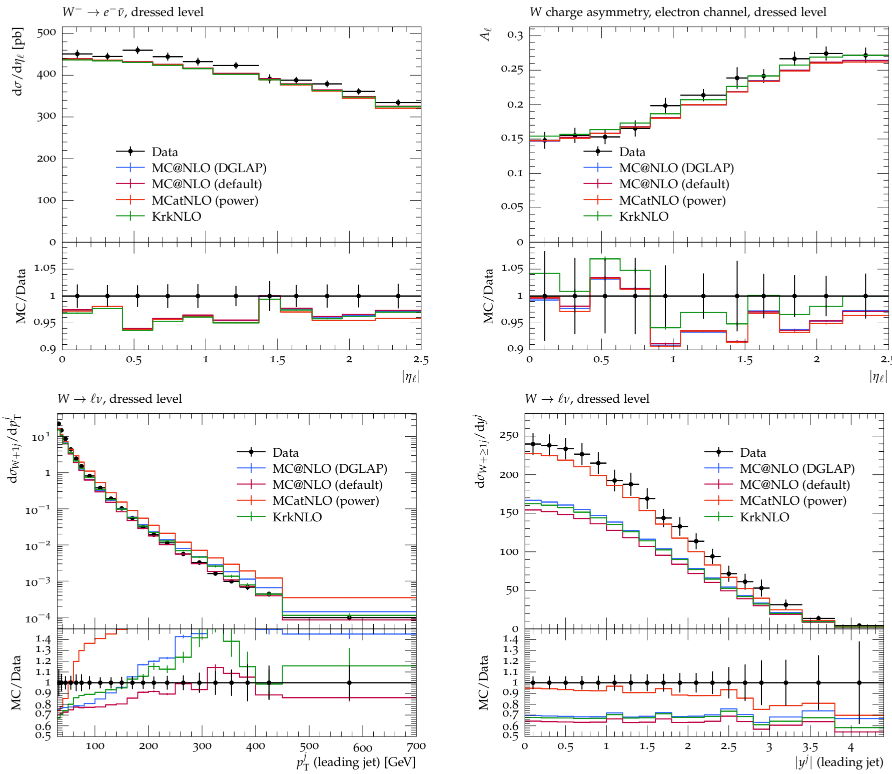

Fig. 3. Comparison of NLO-matched differential distributions generated by KrkNLO and Mc@Nlo at different shower scales to ATLAS data [19, 20].

4. Conclusion

In these proceedings, we have applied the KrkNLO method to the charged-current Drell–Yan process and present phenomenological results comparing the method to the different variations of the Mc@Nlo method. We provide a brief summary of the KrkNLO method followed by a discussion on the phenomenological comparisons. Finally, we compare the methods to data from ATLAS measurements, observing good agreement across different observables — within 5% for those that are formally NLO accurate and within 30–40% for those requiring higher-order corrections to achieve formal NLO accuracy. A detailed study of the phenomenological results of the KrkNLO method for a wider set of observables as well as processes at the LHC will be the subject of a future publication [21].

This work was supported by grant 2019/34/E/ST2/00457 of the National Science Centre (NCN), Poland. A.S. is also supported by the Priority Research Area Digiworld under the program 'Excellence Initiative — Research University' at the Jagiellonian University in Kraków. We gratefully acknowledge Polish high-performance computing infrastructure PLGrid (HPC Center: ACK Cyfronet AGH) for providing computer facilities and support within computational grant No. PLG/2024/016990.

REFERENCES

[1] J. Alwall *et al.*, *J. High Energy Phys.* **2014**, 079 (2014).

[2] F. Buccioni *et al.*, *Eur. Phys. J. C* **79**, 866 (2019).

[3] T. Sjöstrand, S. Mrenna, P.Z. Skands, *J. High Energy Phys.* **2006**, 026 (2006).

[4] C. Bierlich *et al.*, *SciPost Phys. Codeb.* **2022**, 8 (2022).

[5] J. Bellm *et al.*, *Eur. Phys. J. C* **76**, 196 (2016).

[6] J. Bellm *et al.*, *Eur. Phys. J. C* **80**, 452 (2020).

[7] G. Bewick *et al.*, «Herwig 7.3 Release Note», 12, 2023.

[8] T. Gleisberg *et al.*, *J. High Energy Phys.* **2009**, 007 (2009).

[9] E. Bothmann *et al.*, *SciPost Phys.* **7**, 034 (2019).

[10] S. Frixione, B.R. Webber, *J. High Energy Phys.* **2002**, 029 (2002).

[11] P. Nason, *J. High Energy Phys.* **2004**, 040 (2004).

[12] S. Frixione, P. Nason, C. Oleari, *J. High Energy Phys.* **2007**, 070 (2007).

[13] S. Alioli, P. Nason, C. Oleari, E. Re, *J. High Energy Phys.* **2010**, 043 (2010).

[14] S. Jadach *et al.*, *Phys. Rev. D* **87**, 034029 (2013).

[15] S. Jadach *et al.*, *J. High Energy Phys.* **2015**, 052 (2015).

[16] S. Jadach *et al.*, *Eur. Phys. J. C* **77**, 164 (2017).

[17] P. Sarmah, A. Siódmok, J. Whitehead, *J. High Energy Phys.* **2025**, 62 (2025).

[18] S. Jadach *et al.*, *Eur. Phys. J. C* **76**, 649 (2016).

[19] ATLAS Collaboration (G. Aad *et al.*), *Phys. Rev. D* **85**, 072004 (2012).

[20] ATLAS Collaboration (G. Aad *et al.*), *Eur. Phys. J. C* **75**, 82 (2015).

[21] P. Sarmah, A. Siódmok, J. Whitehead, «LHC Phenomenology with KrkNLO», in preparation, 2025.